

# Electrical properties comparison of NTC thermistors prepared from nanopowders and in mixed oxide process

S. M. HOSSEINI, B. GHANBARI SHOHANY\* , N. AZAD, A. KOMPANY

Department of Physics (Materials and Electroceramics Laboratory),  
Ferdowsi University of Mashhad, Iran

We have synthesized and studied the effect of cobalt doping on the electrical properties of NTC thermistors with the composition of  $\text{NiCo}_x\text{Mn}_{2-x}\text{O}_4$  ( $x = 0.0, 0.4, 0.8, 1.2, 1.6$ ). The electrical properties of NTC thermistors prepared from nanopowders by gel auto-combustion and mixed oxides processes have been compared. The measurement results indicate that the fluctuations of B value in the samples made from nanopowders are smaller than that in the samples prepared using mixed oxides method. The electrical properties of these ceramics depend strongly on their grain size. The sintering time and temperature were chosen the same for the samples made from the powders prepared by the two methods. It was found that the samples made from nanopowders have smaller grain sizes.

Keywords: *nanopowders, Ni-Co-Mn, NTC thermistors*

© Wrocław University of Technology.

## 1. Introduction

NTC thermistors, which exhibit a decrease in electrical resistance with increasing temperature, are widely used in manufacturing temperature sensors having negative temperature coefficient. Most ceramic compositions used in NTC thermistors have spinel structure with the general formula  $\text{AB}_2\text{O}_4$ . This structure is based on the oxygen atoms arranged in an fcc structure containing tetrahedral A and octahedral B lattice sites [1].

The electrical conductivity of materials having spinel structure has been explained by small polaron hopping process [2]. The electrical charge transport occurs by hopping of electrons between  $\text{B}^{3+}$  and  $\text{B}^{4+}$  ions present at the octahedral sites in the lattice. The electrical conductivity of  $\text{Mn}_3\text{O}_4$  and similar spinel structures, with  $\text{Mn}^{2+}$  at the tetrahedral sites and  $\text{Mn}^{3+}$  at the octahedral sites, is not very high. This structure does not contain

ions of the same element with different charges at similar sites, as required for electron hopping.

However, the substitution of Mn with Ni or Co increases the conductivity.  $\text{Ni}^{2+}$  occupies octahedral sites and the charge balance is maintained by the conversion of  $\text{Mn}^{3+}$  to  $\text{Mn}^{4+}$ , thus providing a basis for polaron hopping from a  $3d$ -  $\text{Mn}^{3+}$  to a  $3d$ -  $\text{Mn}^{4+}$  both located in the octahedral sites [3].

Fabrication of nanosized NTC precursor powders is of a special interest to sinter fine-grained ceramics. There are several methods for synthesis of the powders such as the mixed oxides [4, 5], ethylene glycol-metal nitrate polymerized complex process [6], co-precipitation with different precipitators [7] and gel auto-combustion process of nitrate-citrate gels [8].

In this work, we have synthesized NTC nanopowders with the compositions of  $\text{NiCo}_x\text{Mn}_{2-x}\text{O}_4$  ( $x = 0.0, 0.4, 0.8, 1.2, 1.6$ ) by gel auto-combustion method. In addition, we employed mixed oxides process in order to compare the performance of these samples.

\*E-mail: boshnags@yahoo.com

The grain size, dependence of resistivity on temperature, material constant (B) and temperature coefficient ( $\alpha$ ) have been measured. Also the microstructure and electrical properties of the samples prepared by gel auto-combustion and mixed oxides methods have been studied and compared.

Despite the number of papers already published on the synthesis of NTC powders and electrical properties of thermistors, the comparison of electrical properties of the compositions prepared by the two methods has rarely been studied. According to our knowledge no experimental results concerning these compositions have been published so far to enable their comparison with the results given in this paper.

## 2. Experimental

### 2.1. Samples prepared from nanopowders

NTC nanopowders were synthesized by gel auto-combustion method. Nickel nitrate -  $[\text{Ni}(\text{NO}_3)_2 \cdot 6\text{H}_2\text{O}]$ , cobalt nitrate  $[\text{Co}(\text{NO}_3)_2 \cdot 6\text{H}_2\text{O}]$ , manganese nitrate  $[\text{Mn}(\text{NO}_3)_2 \cdot 4\text{H}_2\text{O}]$ , citric acid and nitric acid were used as starting materials. According to the presumed composition of  $\text{NiCo}_x\text{Mn}_{2-x}\text{O}_4$ , the appropriate amounts of nitrates, citric acid and nitric acid were dissolved into deionized water to form the mixed solutions. Sol of the NTC was maintained at pH of 7 by adding ammonium hydroxide. The gel was produced by heating the sol at the temperature of about 75 °C.

Finally, the nanopowders of NTC were obtained by adding nitric acid to the gel in order to ignite it. The resultant nanopowders were calcinated at 750 °C to obtain the desired single-phase nanopowders. The calcinated powder was granulated using PVA as a binder, and pressed to form a disk shaped specimen. Then, the disks were sintered at 1200 °C for 6 h in air.

For measuring the electrical properties, the disks obtained from nanopowders were marked as samples A.

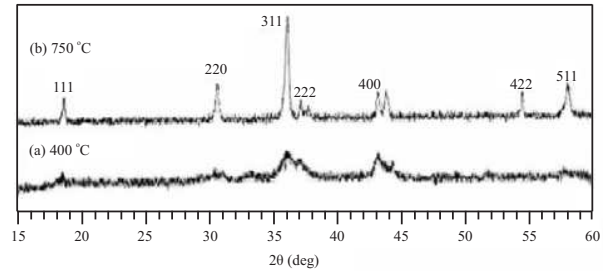


Fig. 1. XRD spectra of the NTC nanopowders calcinated at (a) 400 °C and (b) 750 °C for the composition of  $\text{NiCo}_{1.2}\text{Mn}_{0.8}\text{O}_4$ .

### 2.2. Samples obtained by mixed oxides method

High purity manganese, cobalt and nickel oxides were weighed and mixed according to the presumed composition of  $\text{NiCo}_x\text{Mn}_{2-x}\text{O}_4$  ( $x = 0.0, 0.4, 0.8, 1.2, 1.6$ ). The mixed oxides powders were calcinated at 900 °C. The calcinated powders were granulated, using PVA as a binder, and pressed to form a disk shaped specimen. The samples were sintered at 1200 °C for 6 h in air.

For measuring the electrical properties, the samples made by this method were marked as samples B.

## 3. Results and discussion

### 3.1. Phase analysis and particles size of the samples prepared from nanopowders

The formation of spinel phase has been studied by x-ray diffraction (XRD). Fig. 1 shows the XRD patterns of NTC powders calcinated at 400 °C and 750 °C for the compounds containing high cobalt concentrations ( $\text{NiCo}_{1.2}\text{Mn}_{0.8}\text{O}_4$ ). These patterns were obtained using  $\text{CuK}\alpha$  radiation in the range of 15–60 °. Spinel structure was not completely formed at low calcination temperature (400 °C), but as the temperature increased up to 750 °C the formation of spinel structure took place. The results are consistent with the reports published previously by the others [9, 10].

Fig. 2 shows the XRD patterns for all compounds having different concentrations

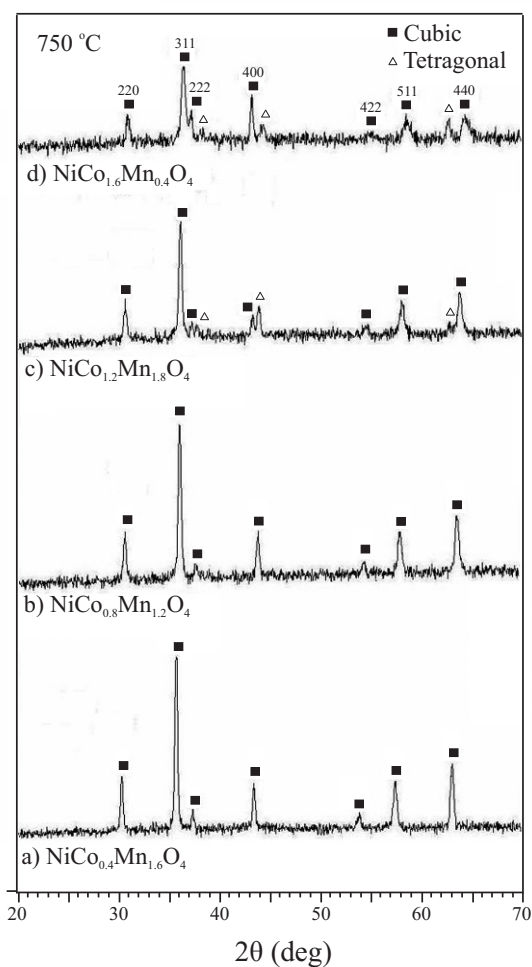


Fig. 2. XRD patterns of four samples of  $\text{NiCo}_x\text{Mn}_{2-x}\text{O}_4$  ( $x = 0.4, 0.8, 1.2, 1.6$ ) system.

of cobalt. The compounds with low cobalt concentrations have a cubic single phase structure, while the samples with high cobalt contents have both cubic and tetragonal structures. The results of calculations also indicate that in the samples with high cobalt concentration, the lattice parameter is smaller. The peak intensity of (311) has been reduced with the increase in cobalt content. However, it seems that the crystallization process of these samples is not very good.

The size of the nanocrystallites was estimated by means of x-ray line broadening method, using Scherrer's formula:  $D = (k\lambda)/(\beta\cos\theta)$ , where  $D$  is the crystallite size,  $\lambda$  is the wavelength of the radiation (1.54056 nm for  $\text{CuK}\alpha$  radiation),  $k$  is

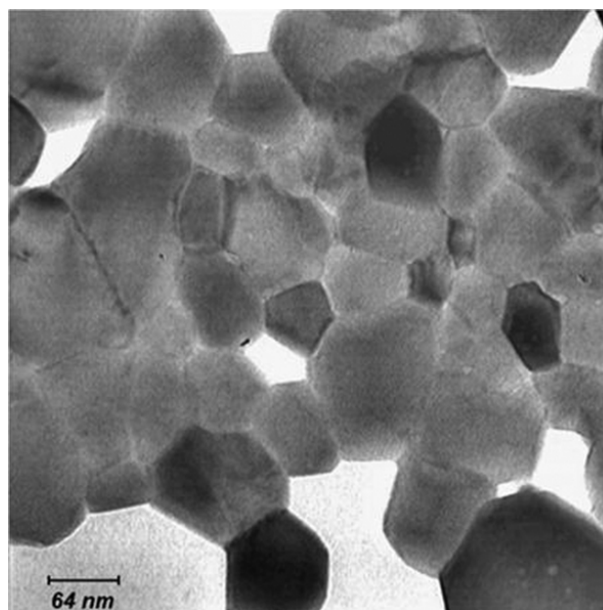


Fig. 3. TEM photograph of the NTC nanopowders in the composition of  $\text{NiCo}_{1.2}\text{Mn}_{0.8}\text{O}_4$  calcinated at  $750\text{ }^\circ\text{C}$ .

a constant equal to 0.94,  $\beta$  is the peak width at half-maximum intensity and  $\theta$  is the peak position.

The results obtained from Scherrer's formula for the nanocrystallites are given in Table 1. In addition, we determined particle size by using transmission electron microscopy (TEM LEO 912B-Germany). The typical TEM image of the particles for the composition of  $\text{NiCo}_{1.2}\text{Mn}_{0.8}\text{O}_4$  calcinated at  $750\text{ }^\circ\text{C}$  is shown in Fig. 3. The geometric figure of the particles is polygon. The average particle size obtained from TEM image is about 65 nm.

### 3.2. Phase analysis of the samples prepared by mixed oxides method

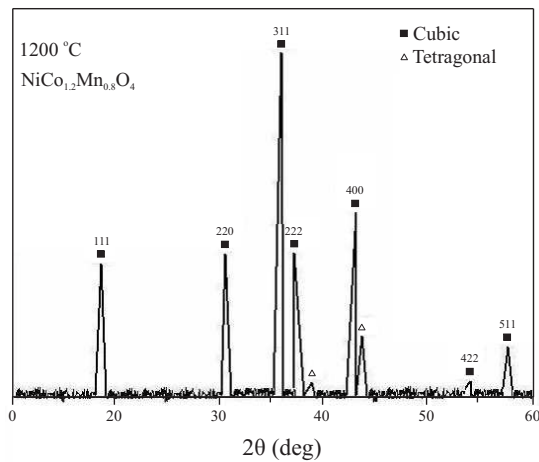
Fig. 4 shows the XRD pattern of the compound having high cobalt concentration, calcinated at  $1200\text{ }^\circ\text{C}$ . This sample presents broader peaks due to the poor crystallization process similar to the sample made from nanopowders. The lattice parameters of both cubic and tetragonal structures are given in Table 2.

Table 1. NTC nanopowders characteristics prepared by gel auto-combustion, calcinated at 750 °C.

Composition	Structure	Lattice constant (nm)	Space group	2θ (deg)	Particle size (nm)
NiCo <sub>0.4</sub> Mn <sub>1.6</sub> O <sub>4</sub>	Cubic	a=0.8333	Fd-3m	30.374, 35.764, 63.103	88 (X-ray)
NiCo <sub>0.8</sub> Mn <sub>1.2</sub> O <sub>4</sub>	Cubic	a=0.8269	Fd-3m	30.675, 36.105, 63.606	82 (X-ray)
NiCo <sub>1.2</sub> Mn <sub>0.8</sub> O <sub>4</sub>	Cubic	a=0.8232	Fd-3m	30.705, 36.134, 63.892	80 (X-ray)
	Tetragonal	a=0.5835, c=0.8423	I41/amd	37.28, 43.44, 63.88	65 (TEM)

Table 2. Lattice parameters for NTC compositions prepared by mixed oxides calcinated at 900 °C.

Composition	Structure	Lattice constant (nm)	Space group
<b>This work</b>			
NiCo <sub>x</sub> Mn <sub>2-x</sub> O <sub>4</sub> (x<1)	Cubic	a=0.83	Fd-3m
NiCo <sub>x</sub> Mn <sub>2-x</sub> O <sub>4</sub> (x>1)	Cubic+Tetragonal	a=0.58, c=0.84	Fd-3m, I41/amd
<b>Others</b>			
NiCo <sub>0.2</sub> Mn <sub>1.8</sub> O <sub>4</sub> [11]	Cubic	a=0.83956	Fd-3m
NiCo <sub>0.7</sub> Mn <sub>1.3</sub> O <sub>4</sub> [11]	Cubic	a=0.83818	Fd-3m
Ni <sub>0.3</sub> Co <sub>1.2</sub> Mn <sub>1.5</sub> O <sub>4</sub> [11]	Cubic+Tetragonal	a=0.58537, c=0.8525	Fd-3m, I41/amd

Fig. 4. XRD pattern of NiCo<sub>1.2</sub>Mn<sub>0.8</sub>O<sub>4</sub> sample prepared from mixed oxides.

### 3.3. Comparison of Electrical properties

The electrical resistance was measured at a constant d.c. voltage with a high-resolution digital voltmeter and the temperature was measured using

a high-resolution (0.1 °C) microprocessor-based digital thermometer, model Fluke-51.

Considering the long-term stability, in the sample with a low nickel content the slow diffusion of nickel occurs from one lattice site to another one. This changes the cations distribution and hence the material constant. As these samples have rather high nickel content, therefore most lattice sites are saturated and only a small amount of nickel atoms may diffuse, which makes the system more stable [12].

The material constant, B, and the temperature coefficient, α, have been evaluated as follows [4]:

$$B = \frac{\ln\left(\frac{\rho_1}{\rho_2}\right)}{\left(\frac{1}{T_1} - \frac{1}{T_2}\right)} \quad (1)$$

$$\alpha = -\frac{B}{T^2} \quad (2)$$

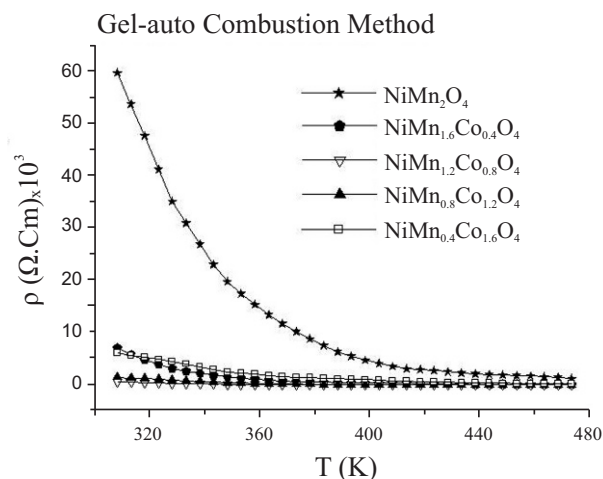


Fig. 5. Variation of NTC resistivity as a function of temperature for the samples prepared by gel auto-combustion process.

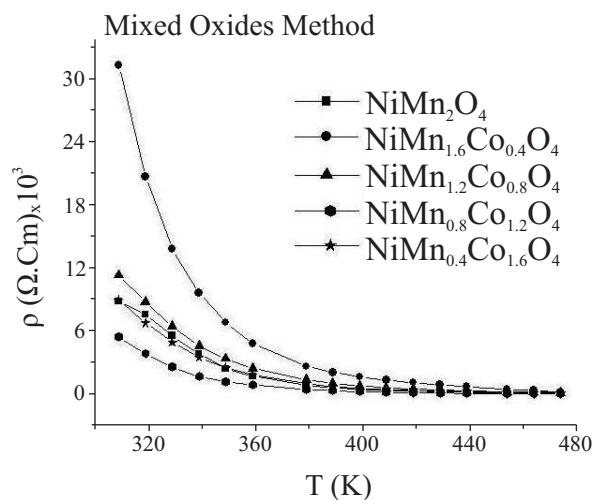


Fig. 6. Variation of NTC resistivity as a function of temperature for the samples prepared by mixed oxides method.

where  $\rho_1$  and  $\rho_2$  are the nominal values of resistivity at  $T_1$  and  $T_2$ , respectively.

Figs. 5 and 6 show the resistivity-temperature response of the samples prepared using gel auto-combustion and mixed oxides methods, between 308 and 473 K. The resistivity of the samples at 308 K varies from 665.1  $\Omega\text{cm}$  for the sample  $\text{NiCo}_{0.8}\text{Mn}_{1.2}\text{O}_4$  to the value of 59877.4  $\Omega\text{cm}$  for the  $\text{NiMn}_2\text{O}_4$  sample.

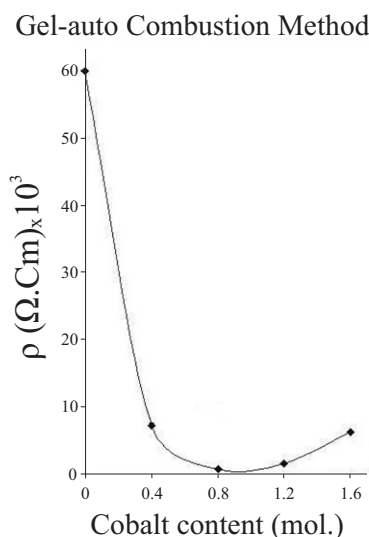


Fig. 7. Variation of d.c. resistivity of the samples prepared from nanopowders as a function of cobalt content ( $T = 308$  K).

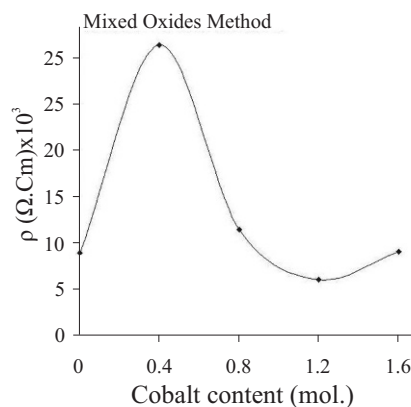


Fig. 8. Variation of d.c. resistivity of the samples prepared by mixed oxides as function of cobalt content ( $T = 308$  K).

Figs. 7 and 8 show the values of d.c. resistivity of the samples as a function of cobalt content at 308 K. For the samples prepared using mixed oxides process, the resistivity of the sample,  $x = 0.4$ , is the highest and decreases with increasing the cobalt content. For the samples prepared by gel auto-combustion route, the resistivity of the sample,  $x = 0.8$ , is minimum and increases when the amount of cobalt in the samples increases.

Table 3. Electrical parameters of NTC thermistors prepared by gel auto-combustion (samples A) and mixed oxides methods (samples B).

Sintering temperature and time	Composition	Material constant B (K)		$\alpha$ [25 °C] ( $10^{-2} \text{ K}^{-1}$ )		Density ( $\text{g/cm}^3$ )	
		Samples A	Samples B	Samples A	Samples B	Samples A	Samples B
<b>This work</b>							
1200 °C, 6 h	NiMn <sub>2</sub> O <sub>4</sub>	3476	4371	-3.92	-4.92	-	-
1200 °C, 6 h	NiCo <sub>0.4</sub> Mn <sub>1.6</sub> O <sub>4</sub>	4283	4408	-4.82	-4.97	5.125	4.72
1200 °C, 6 h	NiCo <sub>0.8</sub> Mn <sub>1.2</sub> O <sub>4</sub>	3620	4130	-4.07	-4.65	5.063	5.059
1200 °C, 6 h	NiCo <sub>1.2</sub> Mn <sub>0.8</sub> O <sub>4</sub>	3455	4367	-3.98	-4.92	5.533	4.83
1200 °C, 6 h	NiCo <sub>1.6</sub> Mn <sub>0.4</sub> O <sub>4</sub>	2851	4141	-3.22	-4.66	5.533	4.688
<b>Others</b>							
1250 °C, 6 h	NiCoMnO <sub>4</sub> [4]	3649		-4.15		Mixed oxides	
1200 °C, 2 h	NiCoMnO <sub>4</sub> [13]	3515-3940		-		Co-precipitation	
1400 °C, 3 h	Mn <sub>(1.75-1.25x)</sub> Co <sub>2.5x</sub> Ni <sub>1.25(1-x)</sub> O <sub>4</sub> (0 ≤ x ≤ 0.6) [14]	3400-4100		-		Mixing Mn, Co and Ni nitrates	
1150 °C,-	Ni <sub>1</sub> Co <sub>0.2</sub> Mn <sub>1.8</sub> O <sub>4</sub> [8]	3350-3360		-		Gel auto-combustion (nitrate-citrate gels)	
- , -	Mn:Co:Ni (45:29:26) [15]	3280		-		Mixed oxides (thick film)	

Since the electrical properties of NTC ceramics strongly depend on the grain size, the using of nanopowders to prepare NTC samples results in smaller grain size at short sintering soak time and hence smaller values of electrical parameters than that of the samples made in mixed oxides process.

The measured values of B and  $\alpha$  for different compositions are summarized in Table 3. The results indicate that the maximum value of B occurs when the content of cobalt is  $x = 0.4$ . Since the electrical properties of these ceramics also depend strongly on the grain size [4], therefore one may expect that the samples made from nanopowders, with smaller grain size, will exhibit smaller value of B, if a short sintering time is chosen. However, in order to improve the electrical parameters of the samples made from nanopowders, in comparison with the samples prepared from mixed oxides, the sintering time needs to be increased, which leads to the increase of the grain size in the sample.

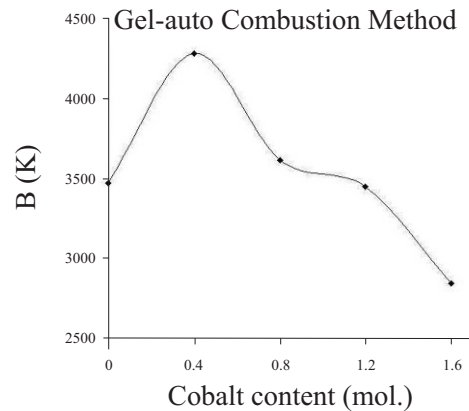


Fig. 9. The material constant, B, as a function of cobalt content for gel auto-combustion samples.

The effect of cobalt content on B constant is shown in Figs. 9 and 10. The results indicate that in both methods, the value of B is maximum for  $x = 0.4$ .

The fluctuation of B values for the samples made from nanopowders is smaller than that of the samples prepared from mixed oxides.

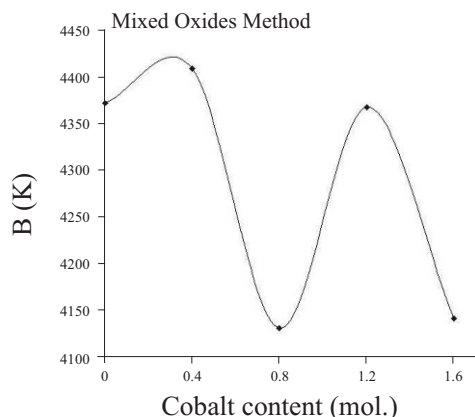


Fig. 10. The material constant, B, as a function of cobalt content for mixed oxides samples.

#### 4. Conclusion

In this paper NTC powders  $\text{NiCo}_x\text{Mn}_{2-x}\text{O}_4$  ( $x = 0.0, 0.4, 0.8, 1.2, 1.6$ ) have been synthesized in gel auto-combustion and mixed oxides processes and the behavior of their electrical properties are compared. The dependence of resistivity on temperature, material constant (B) and temperature coefficient ( $\alpha$ ) have been measured and the results for different samples were also compared. Our results revealed that the fluctuation of B values for the samples made from nanopowders is smaller than that of the samples prepared from mixed oxides. Since the electrical properties of these ceramics depend strongly on the grain size and the samples made from nanopowders have smaller grain size, therefore these samples have smaller value of B and  $\alpha$  in comparison with the mixed oxides samples.

#### References

- [1] BUCHANAN R.C., *Ceramics materials for electronics-processing (edited)*, Marcel Dekker Inc, 1991.
- [2] SCHMIDT R., BASU A., BRINKMAN A.W., *Phys. Rev. B*, 72 (2005), 115101.
- [3] MOULSON A.J., HERBERT J.M., *Electroceramics materials properties applications*, John Wiley and Sons Ltd, 2003.
- [4] HOSSEINI M., YASAEI B., *J. Ceramics International*, 24 (1998), 543.
- [5] FRANCA Y.V., PORFIRIO T.C., MUCCILLO E.N.S., MUCCILLO R., *J. Materials Science Forum*, 530 (2006), 395.
- [6] DURAN P., TARTAJ J., RUBIO F., MOURE C., PENA O., *J. European Ceramic Society*, 24 (2004), 3035.
- [7] MARTIN DE VIDALES J.L., *J. Materials Science*, 33 (1998), 1491.
- [8] WANG W., LIU X., GAO F., TIAN CH., *J. Ceramics International*, 33 (2007), 459.
- [9] ABE Y., MEGURO T., OYAMATSU S., YOKOYAMA T., KOMEYA K., *J. Materials Science*, 34 (1999), 4639.
- [10] YOKOYAMA T., MEGURO T., SHIMADA Y., TATAMI J., KOMEYA K., ABE Y., *J. Mater. Sci.*, 42 (2007), 5860.
- [11] MA Y., BAHOUT M., PENA O., DURAN P., MOUREL C., *Bol. Soc. Esp. Ceram.*, 43 (2004), 663.
- [12] HOSSEINI M., *J. Ceramics International*, 26 (2000), 245.
- [13] ZHUANG J., CHANG A., JIA ZH., ZHUANG SH., JIA D., *J. Ceramics International*, 30 (2004), 1661.
- [14] YOKOYAMA T., MEGURO T., NAKAMURA M., TATAMI J., WAKIHARA T., KOMEYA K., *J. Ceramic Processing Research.*, 10 (2009), 683.
- [15] HUANG J., HAO Y., LIN H., ZHANG D., SONG J., ZHOU D., *Materials Science and Engineering B*, 99 (2003), 523.

Received 2010-05-03

Accepted 2012-01-27